JNeurosci
THE JOURNAL OF NEUROSCIENCE

Research Articles: Behavioral/Cognitive

Computing value from quality and quantity in human decision making

Archy O. de Berker[a,b,c], Zeb Kurth-Nelson[b,e], Robb B Rutledge[a,b], Sven Bestmann[a,c] and Ray Dolan[a,b]

[a]*Wellcome Trust Centre for Neuroimaging, University College London, London WC1N 3BG, United Kingdom*
[b]*Max Planck University College London Centre for Computational Psychiatry and Ageing Research, London WC1B 5EH, United Kingdom*
[c]*Sobell Department of Motor Neuroscience and Movement Disorders, University College London, London WC1N 3BG, United Kingdom*
[d]*Element AI, 4200 St Laurent Boulevard, Montreal, Canada*
[e]*DeepMind, 5 New Street Square, London UK*

https://doi.org/10.1523/JNEUROSCI.0706-18.2018

Received: 18 March 2018

Revised: 20 September 2018

Accepted: 26 September 2018

Published: 19 November 2018

Author contributions: A.O.d.B., Z.K.-N., R.B.R., S.B., and R.J.D. designed research; A.O.d.B., Z.K.-N., and R.B.R. performed research; A.O.d.B., Z.K.-N., R.B.R., and S.B. contributed unpublished reagents/analytic tools; A.O.d.B. and Z.K.-N. analyzed data; A.O.d.B. wrote the first draft of the paper; A.O.d.B., Z.K.-N., R.B.R., S.B., and R.J.D. edited the paper; A.O.d.B., Z.K.-N., R.B.R., S.B., and R.J.D. wrote the paper.

Conflict of Interest: The authors declare no competing financial interests.

Corresponding Author: Archy O. de Berker, archy.deberker@gmail.com, Element AI, 4200 Boul St-Laurent #1200, Montréal, QC H2W 2R2

Cite as: J. Neurosci 2018; 10.1523/JNEUROSCI.0706-18.2018

Computing value from quality and quantity in human decision making

Archy O. de Berker[a,b,c,d], Zeb Kurth-Nelson[b,e], Robb B Rutledge[a,b], Sven Bestmann[a,c], and Ray Dolan[a,b]

[a] Wellcome Trust Centre for Neuroimaging, University College London, London WC1N 3BG, United Kingdom

[b] Max Planck University College London Centre for Computational Psychiatry and Ageing Research, London WC1B 5EH, United Kingdom

[c] Sobell Department of Motor Neuroscience and Movement Disorders, University College London, London WC1N 3BG, United Kingdom

[d] Element AI, 4200 St Laurent Boulevard, Montreal, Canada

[e] DeepMind, 5 New Street Square, London UK

Corresponding Author
Archy O. de Berker
archy.deberker@gmail.com
Element AI, 4200 Boul St-Laurent #1200, Montréal, QC H2W 2R2

Abbreviated Title: Quality and quantity in decision making

Word counts
Abstract: 207
Significance Statement: 107
Introduction: 652
Discussion: 2010

This manuscript comprises 28 pages, with 7 figures (uploaded separately).

AdB was supported by a MRC Studentship. RJD holds a Wellcome Trust Senior Investigator Award (098362/Z/12/Z). The UCL-Max Planck Centre is a joint initiative supported by UCL and the Max Planck Society. The Wellcome Trust Centre for Neuroimaging is supported by core funding from the Wellcome Trust (091593/Z/10/Z). RBR is supported by an MRC Career Development Award (MR/N02401X/1). The authors declare no competing financial interests.

We would like to thank Laurence Hunt and Erie Boorman for fruitful discussion.

Abstract

How organisms learn the value of single stimuli through experience is well described. In many decisions, however, value estimates are computed 'on the fly', by combining multiple stimulus attributes. The neural basis of this computation is poorly understood. Here we explore a common scenario in which decision-makers must combine information about quality and quantity to determine the best option. Using fMRI, we examined the neural representation of quality, quantity, and their integration into an integrated subjective value signal in humans of both genders. We found that activity within Inferior Frontal Gyrus (IFG) correlated with offer quality, whilst activity in the Intra Parietal Sulcus (IPS) specifically correlated with offer quantity. Several brain regions, including the Anterior Cingulate Cortex (ACC), were sensitive to an interaction of quality and quantity. However, the ACC was uniquely activated by quality, quantity, and their interaction, suggesting this region provides a substrate for flexible computation of value from both quality and quantity. Furthermore, ACC signals across subjects correlated with the strength of quality and quantity signals in IFG and IPS respectively. ACC tracking of subjective value also correlated with choice predictability. Finally, activity in the ACC was elevated for choice trials, suggesting that ACC provides a nexus for the computation of subjective value in multi-attribute decision making.

Significance Statement

Would you prefer 3 apples or 2 oranges? Many choices we make each day require us to weigh up the quality and quantity of different outcomes. Using fMRI, we show that option quality is selectively represented in the Inferior Frontal Gyrus (IFG), whilst option quantity correlates with areas of the Intra Parietal Sulcus (IPS) which have previously been associated with numerical processing. We show that information about the two is integrated into a value signal in the Anterior Cingulate Cortex (ACC), and the fidelity of this integration predicts choice predictability. Our results demonstrate how on-the-fly value estimates are computed from multiple attributes in human value-based decision making.

Introduction

Convergent evidence from human fMRI (O'Doherty et al. 2001; Montague and Berns 2002; Kable and Glimcher 2007; Knutson et al. 2007; FitzGerald et al. 2009; Levy et al. 2011) and non-human primate recordings (Schultz et al. 1997; Padoa-Schioppa and Assad 2006; Hayden et al. 2011; Kennerley et al. 2011; Padoa-Schioppa and Schoenbaum 2015) suggest that neural representations of subjective value are present in a wide variety of brain areas, potentially represented in an automatic fashion invariant to the task at hand (Lebreton et al. 2009; Grueschow et al. 2015). These value estimates are thought to provide input to value-comparison mechanisms to enable an appropriate decision between options (Padoa-Schioppa and Assad 2006; 2008; Padoa-Schioppa 2011; Xie and Padoa-Schioppa 2016), a process variously characterized as evidence accumulation (Krajbich et al. 2010; De Martino et al. 2013; Polania et al. 2014) or mutually inhibitory competition (Wang 2008; Hunt et al. 2012; Chau et al. 2014). Representations of stimulus value also plays a crucial role in reinforcement learning, where discrepancies between experienced and expected values give rise to the prediction errors that drive learning (Schultz et al. 1997; Sutton and Barto 1998; Pessiglione et al. 2006; Rutledge et al. 2010; Kahnt et al. 2011).

Despite abundant and consistent evidence for value representations in specific brain areas, we still know little about how they come about and are integrated across multiple attributes. Efforts to isolate value signals within a neuroeconomic framework have used carefully controlled stimulus characteristics and action requirements in an effort to disambiguate value from its components (O'Doherty 2014; Hunt et al. 2015). However, in the real world, we often need to construct valuations of never-before-seen objects. Recent studies using foraging tasks have emphasized that a more ethological contextualization of decision-making provides a richer account of the computations which underlying choice (Cisek and Kalaska 2010; Kahnt et al. 2011; Chau et al. 2014; Kolling et al. 2014), highlighting a need to understand the individual component processes that contribute to value estimation. In this experiment we drew inspiration from such foraging tasks to ask how current option value is constructed from two component parts, quality and quantity.

We designed an experiment where participants integrated information about the quality of a giftcard (how subjectively valuable it was for them to be able to spend money at a particular store) and its quantity (how much money was on the giftcard). In a behavioural session we characterized the combination of quality and quantity to form integrated values using an auction procedure (Becker-DeGroot-Marschak, BDM) (Becker et al. 1964), allowing us to select giftcards with distinct qualities. In the subsequent fMRI experiment, participants evaluated a series of individual giftcards without any choice requirement, allowing us to examine correlates of quality, quantity, and value, that were uncontaminated by decision-related signals (Hunt et al. 2015).

We found that quality was represented in the Inferior Frontal Gyrus (IFG), extending into the lateral PFC. Conversely, quantity was associated with increasing activity in the bilateral Intra Parietal Sulcus (IPS). To identify regions in which the two might be interacting in a manner consistent with the calculation of value, we formulated an explicit interaction term. This interaction term captures the fact that an extra unit of money on the highest *quality* giftcard is more valuable to the subject than an extra unit on the low *quality* giftcard; you would rather have another £ to spend at a shop you really like than at one you dislike. This interaction (higher slope of quantity coding with higher quality) correlated with activity in the posterior cingulate cortex and bilateral superior temporal regions. Anterior Cingulate Cortex (ACC) displayed a conjunction of all three effects, indicative of a substrate for the calculation of integrated subjective value from its component parts. In keeping with this, we also observed repetition suppression for integrated subjective value in the cingulate cortex, with activity covarying with the absolute difference in value between stimuli presented in consecutive trials.

Materials and Methods

Participants

47 participants (25 males) participated in the behavioural study, with 26 returning for an fMRI session. Of these, one participant failed to complete the experiment due to ill-health, leaving 25 participants in total for the imaging study. Both studies were approved by a local ethics committee (Research Ethics Committee UCL, ref. 3450/002). Based on pilot experiments, we selected 13 giftcards that were well known to the participant population, that maximised between-subject variability, and which displayed minimal correlations between cards (i.e. preferences for a given card could not be predicted from preferences for other cards).

During the behavioural session, participants completed two tasks: an auction procedure, from which they could obtain a mixture of up to £20 cash and a £20 giftcard, and a session of paired choices between cards worth £20 (Figure 1). One trial was randomly selected across both sessions and reimbursed appropriately. For the fMRI experiment, participants first completed paired choices between cards worth £20 outside of the scanner, and subsequently chose between cards worth £1-20 within the scanner. One trial from each task was reimbursed, in addition to a £20 flat rate for experiment completion.

Experimental Design and Statistical Analyses

Behavioural session

Participants first performed an auction task (Becker-DeGroot-Marshak, BDM) designed to elicit the subjective valuation of different giftcards holding varying amounts of money (Becker et al. 1964). Briefly, the BDM involves players placing a minimum bid for an item on each trial. After the experiment, a single trial is randomly selected for reimbursement. For that trial, a randomly drawn number – the 'cost' - is compared to the bid. If the cost is higher than the bid, the player retains their endowment and does not receive the item. If the bid is higher than the cost, then the player receives the item, but, crucially, pays the cost rather than their bid. This removes an incentive to place low bids, resulting in an optimal strategy whereby players report their true values. Each of 13 giftcards were presented in association with 12 different quantities, giving a total of 156 trials. Following the auction task, participants chose between pairs of giftcards of matched quantity (£20). Each combination of cards was presented twice, yielding 325 trials after the removal of trials involving two copies of the same card.

We selected a subset of participants to complete the scanning part of the study. Selection was based upon reliability, stability, and diversity of preferences over giftcards. We fit linear regressions to values reported during the auction procedure, yielding the following equation for each giftcard:

$$\text{Integrated Value} = \beta * \text{Quantity} + C$$

Where β and C (an intercept term) were fit using robust regression. The β's thus obtained are a measure of a giftcard's quality, the value of a single unit of currency on that giftcard. We next assessed how well these β's predicted paired choice (Figure 3), selecting subjects for whom there was a close relationship.

For the scanning session, we selected three giftcards, chosen to maximise variance in quality (Figure 3C). We thus selected the lowest and highest quality card (max β and min β), and one closest to the mean of the two. Having performed this selection procedure, we verified that choices of these cards in the paired-choice session reflected the rankings calculated from the BDM (Figure 3). These βs were used as indicators of quality for the fMRI analyses in which parametric modulators were used (GLM2 & GLM3, see below).

115

116 **fMRI task**

117 The task design allowed us to examine representations of quality, quantity, and their interaction, using both linear analyses and measures of
118 repetition suppression. To avoid measurements being confounded by variables related to the dynamics of stimulus comparison (Hunt et al. 2015),
119 on the majority of trials we presented a single stimulus (Figure 1D), and asked participants to evaluate its desirability. Presentation side was flipped
120 every 10 trials. Stimuli remained onscreen for 4000ms, before being followed by an ITI (normally distributed around 1500ms) or, in 1/7 trials, the
121 appearance of a second giftcard. Participants were asked to make a choice between the two within 4000ms, using a button box. Failure to register
122 a choice within this time period resulted in a 'TIME OUT' message, and participants were informed prior to scanning that if a timed-out trial was
123 selected for reimbursement, they would receive no payment for that part of the experiment. Each giftcard displayed in the scanner was pseudo-
124 coloured red or blue to reduce gross visual differences between cards.

125 Repetition suppression in fMRI effects can show sensitivity to expectation (Summerfield et al. 2008), necessitating counterbalancing of stimulus
126 order. We designed our trial presentation order such there was no relationship between the current trial and the next one. This served the dual
127 purposes of avoiding potential confounds in our repetition suppression analysis, and ensuring consistent engagement of our subjects, who were
128 unable to predict when they might have to make a decision.

129 We defined 7 trial types (red and blue versions of each three giftcards, + decision trials), and used a genetic algorithm to find a stimulus order in
130 which $p(stim^j_2|stim^i_1)$ was matched for all stimuli i and j. We manually removed trials on which decisions were repeated, leaving a sequence of 97
131 stimuli. The quantity (1-20) on the giftcards were randomised, effectively orthogonalising quality and quantity (mean correlation coefficient across
132 participants = 0.0074, p= 0.40). Participants completed 4 runs of the task, yielding a total of 340 stimulus evaluation trials and 48 decision trials.

133 **Logistic regression modelling of choices during fMRI task**

134 We used logistic regression to characterize the factors modulating choices in the scanner. For each participant, we fit a model to predict whether
135 they chose the new card (presented during the decision trial), or the old card (on-screen from the valuation trial):

136 $$\text{Choice}(t) = s(\beta_0 + \beta_1 \text{Quality}_{\text{New-Old}} + \beta_2 \text{Quantity}_{\text{New-Old}} + \beta_3 \text{Interaction}_{\text{New-Old}})$$

137 Where β_0 is a constant term accounting for option-independent biases in choice, $\beta_{1\text{-}3}$ are regression coefficients describing the effect of each term
138 on choice, and s is the sigmoid function:

$$s(x) = \frac{1}{1 + e^{-x}}$$

139 Quality was defined using the betas from the BDM auction (see above and Figure 3A), whilst quantity merely reflected the monetary amount (£s)
140 depicted on each giftcard. We formulate the interaction term by first normalizing quality and quantity, and then taking the product.

141 To assess choice predictability, we took the output of the model (valued between 0 and 1), rounded it (such that choices were either a 0 or a 1), and
142 compared it to the vector of actual choices made by the participant. Predictability was then defined simply as the % of choices correctly predicted
143 by the model.

144 **fMRI data acquisition**

145 Data were acquired using a Siemens 3T Trio scanner with a 32-channel head coil at the Wellcome Trust Centre for Neuroimaging. We used a 2D
146 Echo Planar Image (EPI) sequence optimised to minimise dropout in the OFC (Weiskopf et al. 2006), with voxels 3mm isotropic
147 (TR=3.36s,TE=30ms), with 48 slices giving whole brain coverage. Slices were tilted at -30^0. Scans were preceded by a field map (TE1=10ms, TE2=

12.46ms). The first 5 volumes of each run were discarded to allow for T1 equilibration. We also acquired a T1-weighted structural scan for each subject, comprising 176 slices over a field of view of 256mm with a 1mm isotropic resolution (TR=7.92ms, TE=2.48ms) (Deichmann et al. 2004). Throughout scanning, we monitored breathing rate using a pneumatic belt and pulse & blood oxygenation using an infrared pulse oximeter (Nonin systems, Model 8600 F0). Both were digitized and recorded via Spike2 (v6.17), and subsequently included in GLM analyses of brain activity along with regressors derived from motion correction (Hutton 2011).

fMRI data preprocessing

All pre-processing and data analysis took place in SPM12 (http://www.fil.ion.ucl.ac.uk/spm/). Subsequent data visualization took place in MRIcron (http://people.cas.sc.edu/rorden/mricron/index.html) and MRIcroGL (http://www.cabiatl.com/mricrogl/). Having discarding the first 5 volumes, we corrected EPIs for field inhomogeneities using acquired field maps, bias corrected, slice-time corrected (to the middle slice), and realigned and unwarped to the first EPI for each participant. EPIs were then co-registered to each participant's structural scan. We used the DARTEL toolbox for between-subject registration and normalization (Ashburner 2007). Structural images were first segmented into white matter, grey matter, and CSF components. Segmented images were then iteratively warped into normalized MNI space, providing a template that was then used to normalize EPIs, a step which included Gaussian smoothing at 8mm FWHM.

fMRI data analysis

Data were analysed using a series of General Linear Models (GLMs). These were estimated for each participant, including the calculation of contrasts between different regressors (first-level analysis). This provided summary-statistics (βs) which could be tested at a population level versus a null hypothesis that they were on average equal to zero (second-level analysis) (Friston et al. 1999). To obviate multiple comparisons when performing whole brain analyses, we applied a correction using a cluster-defining threshold of $p<0.005$, and a cluster-corrected FWE threshold of $p<0.05$, except for in analysis of repetition suppression (GLM2, below), where a more lenient cluster-forming threshold of $p<0.01$ was used, in line with recent repetition suppression studies (Barron et al. 2013; Garvert et al. 2015; Boorman et al. 2016). To extract the parameter estimates displayed in Figure 5, we used group-functional ROIs thresholded at $p<0.005$. For the conjunction analysis described in Figure 5 we took the product of 3 binary masks (quality, quantity, interaction), each thresholded at $p_{uncorrected}<0.05$, resulting in a family-wise error rate of $p_{uncorrected}=0.000125$.

GLM1: quality and quantity

Our first GLM incorporated separate onset regressors for cards of different qualities (low, medium, high). Each of these was modelled as a 4s long boxcar, and associated with a parametric modulator corresponding to the quantity on the card at each presentation. We used a fourth onset regressor corresponding to decision-trials, which were modelled as delta functions. This GLM was used to perform a whole-brain analysis of value computations during evaluation trials.

We performed three key contrasts:

Quality: $[Quality_{High} - Quality_{Low}]$

Quantity: $[Quantity_{HighQuality} + Quantity_{MediumQuality} + Quantity_{LowQuality}]$

Interaction: $[Quantity_{HighQuality} - Quantity_{LowQuality}]$

The interaction analysis was constructed to test for regions displaying steeper coding of quantity for high quality compared to low quality cards, consistent with value integration. This corresponds to an intuition that an extra unit of a more desirable good (e.g. a Ferrari) is worth more than an extra unit of a less desirable good (e.g. an apple). We excluded trials preceding decisions from the evaluation regressors to guard against contamination of the evaluation regressors by decision-related activity, a possibility arising out of the lack of ITI between evaluation and decision trials.

GLM2: Repetition Suppression

Following the numerosity-coding literature (Piazza et al. 2004; 2007; Jacob and Nieder 2009), we designed a repetition-suppression analysis based upon the absolute change in value between trials (see Figure 7A). We used this analysis to reveal repetition suppression effects within ROIs identified by the whole-brain analysis using GLM1.

$$\Delta\text{IntegratedValue}(t) = |\text{IntegratedValue}(t) - \text{IntegratedValue}(t\text{-}1)|$$

Where IntegratedValue(t) is simply the product of quality and quantity on trial t (as in Equation 5.1). We used a single onset regressor to represent all giftcard presentations, again using a 4s boxcar, with parametric modulators for ΔIntegrated Value, and, as a precaution, Integrated Value. The inclusion of Integrated Value in the model allowed us to confirm that effects of ΔIntegrated Value were not simply the result of spurious correlation with Integrated Value itself. Trials following decisions were excluded as they were preceded by a pair of stimuli, obfuscating calculation of stimulus similarity. As before, we used a second onset regressor for decision trials. Contrasts were calculated merely as the value of the relevant parametric modulators.

GLM3: Integrated Value

In order to obtain a measure of integrated value coding, we used a single 4s boxcar for all evaluation trials, associated with a parametric modulator for integrated value (Quality x Quantity), excluding pre-decision trials as in GLM1. As in GLM1 & 2, decision trials were modelled in a separate regressor with delta onsets. We used this analysis within ROIs identified by the whole-brain analysis in GLM1, to confirm that the ACC region showing a conjunction of quality, quantity, and interaction effects could also be described as coding integrated value.

Statistical tests

Parameter estimates from fMRI are normally distributed, permitting the use of parametric statistics (t-tests and Pearson correlations). When analysing distributions we knew *a priori* to be non-normal (e.g. predictability, which is bounded at 0 and 100), we used non-parametric equivalents (sign-tests and Spearman rank coefficients). All statistical testing was carried out in Matlab.

Results

Behavioural session establishes stable quality estimates

We used a behavioural session to identify participants for whom we could find giftcards with consistently different subjective qualities (Figure 1B). The behavioural session consisted two tasks. Participants (n=47) performed a Becker-DeGroot-Marschak (BDM) auction (Becker et al. 1964) and a series of paired choices, each involving a selection of 13 giftcards (Figure 1C). In the BDM, players reported how much they'd be willing to pay for a giftcard loaded with a certain amount of money, from £1-20. Subsequently, participants made paired choices between different giftcards containing matched sums (£20).

We used a linear fit to the relationship between amount of money on the giftcard and amount bid for each giftcard during the BDM to provide a measure of the quality of each giftcard for each participant (Figure 2A). To maximize power in the fMRI study, we selected subjects whose bids were predictable (Figure 2A) and for whom we could select 3 giftcards with distinct qualities (Figure 2C, circled points in Figure 2B). By way of

confirmation that BDM-estimated values predicted choice, we next compared quality estimates from the BDM with the number of choices of each giftcard in the paired choice session, preferring subjects for whom there was a high correlation (Figure 2B).

Selected subjects thus displayed consistent BDM bids, a high correlation between preferences elicited in the BDM and paired choice sessions, and a low maximum correlation between quality, quantity, and integrated value (Figure 3). Integrated value, calculated as the product of quality and quantity, effectively provided a prediction of the bid a participant would place for a given giftcard. The correlation between quality, quantity, and integrated value reflects the diversity of giftcard qualities. Giftcards with disparate qualities limit the correlation between quantity and integrated value (e.g. Figure 2C, row i and iii), whilst if all giftcards have similar qualities, the quantity/integrated value correlation will be high (Figure 2C, ii).

fMRI experiment: subjects integrate quality and quantity in choice

For each participant in the fMRI experiment (n=25), we used data from the behavioural session to select 3 giftcards: the giftcard that displayed the steepest relationship between BDM bid and quantity (high quality), the giftcard that displayed the lowest (low quality), and a giftcard of intermediate slope (medium quality) (Figure 3A). In a pre-scanning paired choice session, we confirmed that preference estimates from the preceding behavioural session were stable, with subjects making choices between the three selected giftcards in a highly predictable manner (Figure 3B).

Within the scanner, participants made choices between giftcards of varying quality and quantity on 1/7 of trials (Figure 1D), resulting in a total of 48 decisions. Participants remained highly engaged throughout, exceeding the time limit for choice of 4000ms in only 7 of 1200 choices. We used a logistic regression analysis to quantify the impact of differences between the two options upon choice. We calculated an interaction term as the mean-centred product of quality and quantity. Intuitively, the interaction term captures the fact that an extra £ on the highest *quality* giftcard is more valuable to the subject than an extra £ on the low *quality* giftcard. Differences between options in quality, quantity, and their interaction all influenced participants' choices (Quality T_{24}=8.6, $p<0.001$; Quantity T_{24}=13.7, $p<0.001$; Interaction T_{24}=3.8, $p<0.001$) (Figure 3C) implying that participants combined information about quality and quantity to estimate integrated subjective value, rather than considering the two attributes independently.

Brain activity associated with quality, quantity, and their interaction

In the scanner, participants were shown a single giftcard and asked to internally evaluate it (evaluation trials), in the knowledge that they might have to make a fast decision between that option and another (decision trials) (Figure 1D). The preponderance of valuation trials (340/388) provided us with an opportunity to examine value computation in isolation, without potentially confounding effects of decision dynamics (Hunt et al. 2015).

To isolate elements of value representation, we used General Linear Models (GLMs) of voxel-wise brain activity to examine the representation of quality, quantity, and their interaction in valuation trials. We split card presentations by quality (low, medium, high), and associated each onset with a parametric modulator corresponding to the quantity presented on that trial. This allowed us to index main effects of card quality, [$Quality_{High}$ - $Quality_{Low}$], card quantity [$Quantity_{LowQuality}$ + $Quantity_{MediumQuality}$ + $Quantity_{HighQuality}$], and the interaction between the two [$Quantity_{HighQuality}$ - $Quantity_{LowQuality}$].

The interaction term allows us to identify regions where quantity affects activity more when giftcard value is high compared to when it is low. By decomposing value in this way – into quality, quantity, and their interaction – we can identify brain regions displaying specific relationships with each component, as well as regions showing an overlap of all three effects. This conjunction analysis is more stringent than a simple contrast for integrated value, because it prevents erroneously identifying regions which simply have a strong correlation with only quality or quantity. Motivated by this same logic, recent studies formulate fMRI contrasts for Reward Prediction Errors (RPEs) as a conjunction of positive coding for

reward and negative coding for reward expectation, thus avoiding false positives arising from the correlation between RPEs and other variables such as reward itself (Rutledge et al., 2010).

We found three largely non-overlapping patterns of response corresponding to the representation of offer quality, quantity, and their interaction. Higher card quality was associated with greater activity in bilateral Inferior Frontal Gyrus (IFG), centred on the pars opercularis (Left: Peak MNI= -54, 12, 30; T_{24}=4.79, $p_{FWE\text{-}corrected}$=0.023; Right: Peak MNI= 51, 9, 27; T_{24}=4.37, $p_{FWE\text{-}corrected}$=0.032) (Figure 4A). On the left, this extended into dorsolateral PFC (Peak MNI= -36, 48, 24; T_{24}=3.16, $p_{FWE\text{-}corrected}$=0.044) and included Broca's area, an area associated with semantic comprehension (Price 2012), arguably a process necessary for evaluating abstract stimuli such as giftcards. Parameter estimates extracted from group-level functional ROIs within IFG (defined at p<0.005) suggested an absence of sensitivity to either quantity (T_{24}=1.18,p=0.24), or the interaction of quantity and quality (T_{24}=1.53, p=0.14) in this region, although direct comparisons did not distinguish quality coding from that of quantity or the interaction (T_{24}=1.88,p=0.073; T_{24}=1.88,p=0.17).

Offer quantity correlated with activity in bilateral Intraparietal Sulcus (IPS) (Left: Peak MNI: -27,-66,51; T_{24}=4.77, $p_{FWE\text{-}corrected}$<0.001; Right: Peak MNI: 33,-66,51; T_{24}=4.68, $p_{FWE\text{-}corrected}$<0.001) resonating with a role for this region in numerical reasoning in humans and non-human primates (Nieder and Miller 2004; Piazza et al. 2004; Pinel et al. 2004; Piazza et al. 2007; Harvey et al. 2013)(Figure 4B). As for IFG, activity in the IPS was selective for number, with no sensitivity to quality (T_{24}=0.19, p=0.85) or the interaction of quality and quantity (T_{24}=0.84, p=0.41). This indicates IPS is not performing value coding per se, but specifically represents quantity of available options. Direct comparisons confirmed that quantity correlations were greater than those for quality (T_{24}=3.52, p=0.0017) and for the interaction (T_{24}=3.36,p=0.0025). We also observed quantity-related activity in bilateral visual cortex (Left: Peak MNI: -33,-87,-12; T_{24}=5.54, $p_{FWE\text{-}corrected}$<0.001; Right: Peak MNI: 27,-87,-12; T_{24}=5.49, $p_{FWE\text{-}corrected}$<0.001)

Finally, we asked whether activity in any region of the brain was associated with an interaction between quality and quantity, correlating more steeply with quantity for high compared to low quality giftcards. This is a signature of value computation, involving additional processing above and beyond a simple reflection of option quality or quantity. The most prominent effect was located along the posterior cingulate cortex (Peak MNI: -12,-15,54; T_{24}=3.57, $p_{FWE\text{-}corrected}$<0.001) where activity was specific to the interaction term, with no evidence of quality (T_{24}=-0.14,p=0.89), or quantity (T_{24}=0.77, p=0.45) correlations, implying that despite this region's involvement in value computation it does not represent an integrated value signal *per se*. Direct comparisons confirmed that the interaction effect exceeded both quality (T_{24}=2.93,p=0.0072) and quantity (T_{24}=2.53,p=0.018) contrasts. Interaction contrast effects were also present in bilateral superior temporal lobes (Left: Peak MNI=-63,-45,0; T_{24}=5.55, $p_{FWE\text{-}corrected}$<0.001; Right: Peak MNI=48,-33,3; T_{24}=4.85, $p_{FWE\text{-}corrected}$<0.001)(Figure 4C).

Computation of integrated value from component parts in the cingulate

Having characterized neural responses to individual components of option value (quality, quantity, and their interaction), we next asked whether any regions represented integrated value. To do so, we formulated a parametric regressor for subjective integrated value, by combining quality and quantity mutliplicaively in the manner suggested by our behavioural results (Figure 3).

However, since integrated value is correlated with quality and quantity (though this correlation is limited by design) testing for effects of integrated value presents a problem as regions sensitive to quality or quantity alone might appear to reflect integrated value. To overcome this, we supplemented our parametric analysis with a conjunction analysis, reasoning that a region truly representing integrated value ought to display sensitivity to all of its component: quality, quantity, and their interaction. Importantly, the interaction of two mean-centred variables is decorrelated from either component, giving us a way to check for correlates of *computation* of subjective value.

Both analyses revealed a striking convergence on the anterior cingulate cortex (ACC) (Figure 5) where activity covaried with a parametric modulator for integrated value (Peak MNI: -12,21,39; T_{24}=6.04, $p_{FWE\text{-}Corrected}$<0.001) and showed a conjunction of effects of quality, quantity, and their interaction (all $p<0.05_{uncorrected}$). This chimes with known roles of this regions, including the fact that it contains neurons that multiplex attributes in value-based decision-making (Kennerley et al. 2011) and its necessity for value-learning (Rushworth and Behrens 2008; Hayden et al. 2009). Decomposing the interaction effect within the ACC, we observed that although quantity coding for all three qualities was positive, it was only significantly so in the high quality condition ($Quantity_{LowQuality}$: T_{24}=0.15, p=0.87; $Quantity_{MidQuality}$: T_{24}=1.51, p=0.14; $Quantity_{HighQuality}$: T_{24}=4.24, p<0.001). By way of comparison, all three of these effects were significant in the IPS region pictured in Figure 4B, with no significant difference between coding of quantity for high and low quality giftcards ($Quantity_{LowQuality}$: T_{24}=2.30, p=0.03; $Quantity_{MidQuality}$: T_{24}=2.69, p=0.012; $Quantity_{HighQuality}$: T_{24}=4.78, p<0.001; $Quantity_{HighQuality}$ vs. $Quantity_{LowQuality}$: T_{24}=1.17, p=0.25).

We next reasoned that if the ACC's value estimates guide choice then we should see greater activity in decision trials compared to valuation trials. This was indeed the case with decision trials associated with enhanced activity in the same region (Peak MNI=9,15,45; T_{24}=17.03, $p_{FWE\text{-}Corrected}$<0.001) (Figure 5B). Dorsally, this region overlaps with activity in dmPFC showing an integrated value difference signal (Lebreton et al. 2009; Grueschow et al. 2015) and previously characterized as the final value-comparison step prior to motor output (Hare et al. 2011).

Our analyses revealed dissociable representations of quality, in the IFG, and quantity, in the IPS. Although we lack the temporal precision to test whether these segregated representations precede the emergence of integrated value signals in ACC, we nevertheless can ask whether between-subject variability in component coding is related to between-subject variability in ACC representations. We found evidence that this was the case, with stronger IFG encoding of quality was associated with stronger coding of quality in ACC (r=0.63, p<0.001) (Figure 5C), whilst stronger IPS encoding of quantity was associated with stronger quantity coding in the ACC (r=0.68, p<0.001) (Figure 5F). Importantly, the converse correlations did not hold, with parameter estimates for IGF quality unrelated to ACC quantity (r=0.04, p=0.83) and IPS quantity unrelated to ACC quality (r=0.14, p=0.50) coding (Figure 5D, 5E). This specificity suggests that observed correlations reflect meaningful inter-regional relationships rather than correlated variance in signal-to-noise between participants.

Strength of neural quantity coding reflects choice predictability

The degree to which subjects' choices were correctly predicted by our logistic regression varied, from 69% to 92%. We reasoned that stronger neural representations of value components should lead to more predictable choices. Using parameter estimates (β's) extracted from our GLM analyses, we asked whether between-subject variability in β's related to between-subject choice predictability. We found that the strength of neural correlations with quantity, but not quality, were associated with predictability of choice (Figure 6). Mean β's in both the IPS (ρ=0.60, p=0.002) and ACC (ρ=0.42, p=0.039) were positively correlated with choice predictability, suggesting that stronger neural representations of quantity correspond to more reliable choices. Correlations between predictability and quality coding in the IFG (ρ=0.41, p=0.104) and ACC (ρ=0.30, p=0.142) were also positive but did not reach significance, perhaps reflecting the greater range of values for quantity than quality or the potential impact of overtraining on giftcard quality. We observed no relationship between interaction-coding in ACC and predictability (ρ=-0.04, p=.83). We note that applying a conservative Bonferroni correction for the 5 comparisons we make here, only the effect in the IPS survives an adjusted threshold of α=0.01.

Using summed log-likelihood of choices according to the logistic regression model as an alternative measure of choice predictability yielded a consistent pattern of results, although the effect in the ACC was no longer significant at α=0.05 (IPS: ρ=0.55, p=0.004; ACC: ρ=0.35, p=0.089). We did not observe any other correlations between the parameters of our logistic regression model for behaviour and those of our GLMs for neural activity.

Repetition suppression for integrated value in the ACC

Repetition Suppression (RS) describes the phenomenon whereby repeated presentation of stimuli that are similar along some dimension evoke reduced activity in brain regions sensitive to that attribute (Grill-Spector et al. 2006). This is putatively due to a reduction in activity in neurons activated in both trials (Figure 7). This provides a means to assay the neural overlap in the representation of two stimuli such as foods (Barron et al. 2013), faces (Loffler et al. 2005) or even agents (Garvert et al. 2015). This can reveal non-monotonic codes invisible to traditional GLM approaches, such as tuned numerosity representations in the parietal cortex (Piazza et al. 2004; 2007; Jacob and Nieder 2009). Since our task involved the calculation of value from information about quantity, we hypothesized that value representations in the ACC might show a similar form.

We asked whether RS provides additional evidence of value encoding in ACC. We constructed a GLM where we modelled the absolute difference in integrated value (ΔIntegratedValue) between subsequent trials, as well as the Integrated Value on each trial. If neurons in a brain region are undergoing RS, aggregate activity as assayed by BOLD should covary with the absolute difference between trials (Barron et al. 2016). We found evidence for repetition suppression to value in dorsal ACC (Peak MNI: -3,3,51; T_{24}=3.86, $p_{FWE\text{-}Corrected}$=0.003), just posterior to the activity related to monotonic encoding of integrated value (Figure 7B). These activations were partially overlapping, such that the integrated-value coding conjunction identified in Figure 5 showed effects of both ΔIntegratedValue and Integrated Value (Figure 7C) (ΔIntegratedValue: T_{24}=2.48, p=0.020; Integrated Value: T=3.26, p=0.0034). Repetition suppression for integrated value was surprisingly widespread. We also observed repetition suppression for value bilaterally in the lingual gyrus (Left: Peak MNI: -15,-45,-9; T_{24}=6.18, $p_{FWE\text{-}Corrected}$<0.001; Right: Peak MNI: 15,-48,3; T_{24}=4.56, $p_{FWE\text{-}Corrected}$<0.001), the right superior temporal sulcus (Peak MNI: 63,-30,3; T_{24}=5.80, $p_{FWE\text{-}Corrected}$<0.001), and bilaterally in the posterior insula (Left: Peak MNI: -30,0,-3; T_{24}=5.00, $p_{FWE\text{-}Corrected}$<0.001; Right: Peak MNI: 33,-6,-12; T_{24}=3.60, $p_{FWE\text{-}Corrected}$<0.001)

Discussion

Value representations are often studied as monolithic entities. Indeed, considerable effort has been expended in identifying abstract behavioural and neural signatures of scalar value estimates. However, recent work suggests that during choice, components of value compete at an attribute-level to guide decisions (Hunt et al. 2014), emphasising the importance of decomposing value into its constituent parts. Here we show that in the absence of choice, integrated value correlates appear in the ACC, with component representations in the IFG (quality), and IPS (quantity) (Figures 5 & 6). A distinct network appears to integrate the two, with posterior cingulate and superior temporal lobe activations corresponding to the interaction between quality and quantity (Figure 4). A more posterior region of the ACC displays repetition suppression to integrated value (Figure 7).

Correlates of quality and quantity in the brain

Bilateral IFG activity scaled with the quality of the giftcard presented on each trial (Figure 4A). This was unexpected, given the scarcity of reports of IFG involvement in value-based decision making (though see (Rogers et al. 1999; Zysset et al. 2006; Liljeholm et al. 2011)). *A priori*, the orbitofrontal cortex (OFC) might represent a more promising candidate for the representation of stimulus quality. However, representations in the OFC appear to be particularly entangled with stimulus identity (Padoa-Schioppa and Assad 2008; Barron et al. 2013; Klein-Flügge et al. 2013; McNamee et al. 2013; Howard et al. 2015, Noonan et al. 2011), potentially reflecting the central role of the OFC in providing an internal model of the world (Wilson et al. 2014). For instance, Padoa-Schioppa and Assad (2008) describe OFC cells that respond specifically to one juice or another, which they describe as reflecting the *taste* of a given juice. This encoding of juice *identity* is distinct from the reward *quality*, and no study has reported OFC unit responses that reflect quality alone (i.e., the preference ordering of different stimuli), while being insensitive to quantity. It seems, therefore, that the OFC is particularly interested in tracking *relationships* between specific rewards and their predictors (Takahashi et al. 2013; Stalnaker et al. 2014; Lopatina et al. 2015; Lucantonio et al. 2015; Stalnaker et al. 2015; Boorman et al. 2016, Noonan et al., 2011), rather than estimating stimulus quality per se. Furthermore, a recent study found that OFC *exclusively* represented hidden variables related to the current

state (Schuck et al. 2016). The lack of OFC involvement in our task is likely to reflect the static and transparent relationship between stimuli and outcomes in our experiment.

The involvement of the IFG in the representation of stimulus quality is consistent with the semantic nature of the giftcard stimuli we used. IFG is commonly activated in lexical tasks (Price 2012), with left-hemisphere lesions to this area producing impairments in language production and comprehension. In one of the few studies attempting to parse value into distinct components, Lim et al (Lim et al. 2013) offered participants t-shirts that varied in their aesthetic and semantic properties. They found correlations with aesthetic value in the fusiform gyrus and semantic value in the superior temporal gyrus, whilst vmPFC activity correlated with the value of both attributes. This suggests that the extraction of quality may occur in concert across brain areas specialized for the analysis of distinct stimulus features, in the same way that feedforward models of visual inputs eventually produce value estimates in deep reinforcement learning networks (Mnih et al. 2015; Silver et al. 2016). This suggests that a representation of stimulus quality in IFG may be specific to semantically rich stimuli, such as those employed here.

Conversely, our observation of quantity coding in the IPS (Figure 4B) is predicted from the literature (Nieder 2016). A wide variety of animals show an ability to make ethologically relevant decisions using number, from lions (McComb et al. 1994), to crows (Rahman et al. 2014) . Even new-born chicks are capable of tracking the number of an imprinted object that is placed behind a screen (Rugani et al. 2009). In macaques, such judgments rely upon a network of frontal and parietal regions containing neurons tuned to different numbers, including the number zero (Nieder et al. 2002; Nieder and Miller 2004; Ramirez-Cardenas et al. 2016).

Studies in humans have made use of model-based decoding analyses (Harvey et al. 2013) and repetition suppression designs (Piazza et al. 2004; 2007; Jacob and Nieder 2009) to provide evidence that similar tuning curves for number exist in the human intraparietal sulcus (IPS). Our results imply that the same IPS circuitry subserves number representation in value computation. This is consistent with the recent observation that when number and value are decorrelated, the IPS tracks quantity and not value (Kanayet et al. 2014). This serves to clarify the role of parietal cortices in value-based decision making, suggesting that when financial stimuli are used (Ballard and Knutson 2009; Clithero et al. 2009; Chau et al. 2014), evaluation occurs within a financial framework (such as the BDM) (Plassmann et al. 2007; Medic et al. 2014), or if stimuli merely differ in magnitude (Louie et al. 2011), parietal responses to quantity may be misconstrued as representing value or its comparison. Conversely, we find that the IPS specifically represents the quantity of an available option, and that the strength of numerical representations in IPS correlates both with choice predictability and ACC quantity coding. This is consistent with neurons in IPS contributing to the representation of stimulus value in the ACC, and this latter representation subsequently being used to guide choice. However, it is unclear why choice predictability is so much strongly linked to quantity coding than it is to quality coding (in IFG and ACC) and to interaction coding (in the ACC). We suspect that the greater range of quantities than qualities in our experiment may have increased our power to observe relationships with quantity coding, but this remains an open question.

The role of the ACC in evaluation

We found that activity in the ACC was consistent with representation of integrated value. ACC showed a positive correlation with integrated value. Even after accounting for the effects of quality and quality, ACC tracked the interaction term characteristic of integrated value in this task (Figures 5C and 6A). Beckmann et al (Beckmann et al. 2009) parcellated the cingulate cortex according to connectivity. The region we identify corresponds to their region 4, which shows strong connectivity to dorsolateral prefrontal cortex, and is commonly implicated in value-based tasks. The region showing repetition suppression effects may be more situated in their region 5, which has a higher connectivity to the parietal cortex. This raises the possibility that the repetition suppression we observe is inherited from tuned numerical representations in parietal cortex (Nieder and Miller 2004).

The ACC is frequently identified in both human (Bush et al. 2002; Kolling et al. 2012; Boorman et al. 2013) and animal experiments (Seo and Lee 2007; Hayden et al. 2009; Hayden and Platt 2010; Kennerley et al. 2011; Cai and Padoa-Schioppa 2012) of value-based choice. The more dorsal region in which we find signatures of integrated value is associated with tasks wherein participants assign value to actions (Beckmann et al. 2009). This is the case in our experiment, since giftcards were displayed either on the left or the right hand side of the screen, such that assessing the value of a particular giftcard was the same as assessing the value of a left/right button press. Dorsal ACC appears to be particularly engaged by foraging type tasks, in which the pertinent comparisons are between options presented sequentially (Seo and Lee 2007; Kolling et al. 2012; Boorman et al. 2013). We further note that since the positive value correlations we observe in the ACC are recorded in the absence of choice, they cannot be explained as a function of choice difficulty and are more consistent with a proposed role in sequential foraging decisions (Kolling et al., 2016).

We did not observe value-related activity in the ventromedial PFC (vmPFC), the part of the cortex most frequently associated with valuation (Rushworth and Behrens, 2008), nor in the ventral striatum. This chimes with recent observations suggesting that sequential (Hunt et al., 2013) or time-limited (Jocham et al., 2014) choices do not engage vmPFC. Indeed, a growing body of evidence suggests that the ACC is particularly when subjects engage in sequential, foraging-type decisions, characterized by an evaluation of whether to engage or not (Kolling et al., 2012, Kolling et al., 2016). Conversely, whether evaluation alone effectively engages vmPFC is unclear. Although early reports suggested that the vmPFC was part of an automatic valuation system (Lebreton et al., 2009), recent work suggests otherwise (Grueschow et al., 2015). The few studies that report value-related activity in macaque vmPFC do so in the context of free viewing (Abitbol et al, 2015; Strait et al., 2014), raising the possibility that the vmPFC is particularly engaged when values are compared via repeated eye movements (Krajbich et al., 2010). The observation that vmPFC is crucial for episodic memory and imagination (Benoit et al., 2014, Hassabis and Maguire, 2009), and a predominance of saccade-frequency theta oscillations in mPFC (Adhikari et al., 2010, Paz et al., 2008), hints at a more general role for the vmPFC in mediating a short-term plasticity allowing features – of a scene, an episode, or a choice – to be integrated over several seconds. This might explain why our task, which required participants to evaluate a single stimulus at a single location, did not modulate vmPFC activity.

Our finding that the cingulate cortex integrates information about quality and quantity to form a multiplicative value representation of the current stimulus is also interesting in light of a literature implicating the cingulate in the representation of values associated with 'model-based' cognition (Wunderlich et al. 2012; Doll et al. 2015). This describes flexible computation of value associated with a certain stimulus, and is typically contrasted with 'model-free' cognition, in which stimulus or action values are cached and updated only through repeated experience (Dolan and Dayan 2013). The multiplication of quantity and quality we observe in the ACC is consistent with the idea that the cingulate provides a model which produces estimates of quantities relevant to behavior (O'Reilly et al. 2013; Economides et al. 2014; Kolling et al. 2014). In our case, utility was maximized by combining quality and quantity in a multiplicative manner, and this is what the ACC appears to do, in a manner that reflects the coding of quality and quantity in the frontal and parietal lobes respectively (Figure 5 C,F).

Our design also enabled us to perform a repetition suppression analysis, allowing us to reveal coding schemes hidden to conventional BOLD analyses. We found that parts of the cingulate cortex displayed repetition suppression to integrated value, with activity that scaled with the absolute difference in value between trials (Figure 7A). This region was posterior to the peak activity associated with monotonic integrated value, extending into the area identified in the conjunction analysis of quality, quantity, and their interaction (Figure 7B). Although the precedent from the numerosity-coding literature is to suppose that RS results of this kind provide positive evidence of non-monotonic tuning (Piazza et al. 2004; Ansari and Dhital 2006; Piazza et al. 2007; Jacob and Nieder 2009), we are cognisant such repetition suppression effects are not an unambiguous signature of non-monotonic codes. In modelling work to be reported elsewhere, we observe that repetition suppression effects such as the ones we observe here can result from mixed linear codes combined with divisive adaptation. Furthermore, given the role of the ACC in comparing option values over time (Kolling et al., 2012; Kolling et al., 2014), the observed relationship with variance in value from trial-to-trial could reflect a

cognitively-meaningful surprise signal, potentially related to environmental volatility (Behrens et al., 2007). Recent work observes just such a signal in a biophysically plausible model of reward learning, in which learning is adapted to volatility via metaplasticity (Farahashi et al., 2017).

To conclude, we find that a distributed network comprising the intraparietal sulcus, inferior frontal gyrus, and posterior cingulate and superior temporal sulcus contribute to the computation of integrated value in the ACC. The strength of signals in the ACC reflected the degree to which they were represented in brain areas coding for quality (lFG) and quantity (IPS), and stronger brain correlations with quantity were associated with more predictable choices. We further demonstrate that parts of the ACC also show repetition suppression to integrated value, consistent with the idea that tuning for value is non-monotonic in parts of the cortex. Our findings demonstrate how value is assembled from its component parts, and emphasise the potential for repetition suppression as an assay of population encoding scheme.

References

Abitbol, R., Lebreton, M., Hollard, G., Richmond, B. J., Bouret, S., & Pessiglione, M. Neural mechanisms underlying contextual dependency of subjective values: converging evidence from monkeys and humans. The Journal of Neuroscience. 2015 Feb 4; 35(5), 2308–2320.

Adhikari, A., Topiwala, M. A., & Gordon, J. A. Synchronized activity between the ventral hippocampus and the medial prefrontal cortex during anxiety. Neuron. 2015 Jan 28; 65(2), 257–269.

Ansari D, Dhital B. Age-related Changes in the Activation of the Intraparietal Sulcus during Nonsymbolic Magnitude Processing: An Event-related Functional Magnetic Resonance Imaging Study. J Cogn Neurosci. 2006 Nov;18(11):1820–8.

Ashburner J. A fast diffeomorphic image registration algorithm. Neuroimage. 2007 Oct 15;38(1):95–113.

Ballard K, Knutson B. Dissociable neural representations of future reward magnitude and delay during temporal discounting. Neuroimage. 2009 Mar 1;45(1):143–50.

Barron HC, Dolan RJ, Behrens TEJ. Online evaluation of novel choices by simultaneous representation of multiple memories. Nature Neuroscience. 2013 Oct;16(10):1492–8.

Barron HC, Garvert MM, Behrens TEJ. Repetition suppression: a means to index neural representations using BOLD? Philosophical transactions of the Royal Society of London Series B, Biological sciences. 2016 Oct 5;371(1705).

Becker GM, DeGroot MH, Marschak J. Measuring utility by a single-response sequential method. Behav Sci. 1964 Jul;9(3):226–32.

Beckmann M, Johansen-Berg H, Rushworth MFS. Connectivity-based parcellation of human cingulate cortex and its relation to functional specialization. J Neurosci. 2009 Jan 28;29(4):1175–90.

Behrens, T. E. J., Woolrich, M. W., Walton, M. E., & Rushworth, M. F. S. Learning the value of information in an uncertain world. Nature Neuroscience. 2007 Sep 1; 10(9), 1214–1221.

Benoit, R. G., Szpunar, K. K., & Schacter, D. L. Ventromedial prefrontal cortex supports affective future simulation by integrating distributed knowledge. Proceedings of the National Academy of Sciences. 2014 Nov 18; 111(46), 16550–16555.

Boorman ED, Rajendran VG, O'Reilly JX, Behrens TE. Two Anatomically and Computationally Distinct Learning Signals Predict Changes to Stimulus-Outcome Associations in Hippocampus. Neuron. 2016 Mar 16;89(6):1343–54.

Boorman ED, Rushworth MF, Behrens TE. Ventromedial prefrontal and anterior cingulate cortex adopt choice and default reference frames during sequential multi-alternative choice. J Neurosci. 2013 Feb 6;33(6):2242–53.

Bush G, Vogt BA, Holmes J, Dale AM, Greve D, Jenike MA, et al. Dorsal anterior cingulate cortex: a role in reward-based decision making. Proc Natl Acad Sci USA. 2002 Jan 8;99(1):523–8.

C Hutton OJJSEFAROSJBNW. The impact of physiological noise correction on fMRI at 7 T. Neuroimage. Elsevier; 2011 Jul 1;57(1-4):101.

Cai X, Padoa-Schioppa C. Neuronal encoding of subjective value in dorsal and ventral anterior cingulate cortex. J Neurosci. 2012 Mar 14;32(11):3791–808.

Chau BKH, Kolling N, Hunt LT, Walton ME, Rushworth MFS. A neural mechanism underlying failure of optimal choice with multiple alternatives. Nature Neuroscience. Nature Publishing Group; 2014 Feb 9;17(3):463–70.

472 Cisek P, Kalaska JF. Neural mechanisms for interacting with a world full of action choices. Annual Review of Neuroscience. 2010;33:269–98.

473 Clithero JA, Carter RM, Huettel SA. Local pattern classification differentiates processes of economic valuation. Neuroimage. 2009 May 1;45(4):1329–38.

474 De Martino B, Fleming SM, Garrett N, Dolan RJ. Confidence in value-based choice. Nature Neuroscience. 2013 Jan;16(1):105–10.

475 Deichmann R, Schwarzbauer C, Turner R. Optimisation of the 3D MDEFT sequence for anatomical brain imaging: technical implications at 1.5 and 3 T. Neuroimage.
476 2004 Feb;21(2):757–67.

477 Dolan RJ, Dayan P. Goals and habits in the brain. Neuron. 2013 Oct 16;80(2):312–25.

478 Doll BB, Duncan KD, Simon DA, Shohamy D, Daw ND. Model-based choices involve prospective neural activity. Nature Neuroscience. 2015 May;18(5):767–72.

479 Economides M, Guitart-Masip M, Kurth-Nelson Z, Dolan RJ. Anterior cingulate cortex instigates adaptive switches in choice by integrating immediate and delayed
480 components of value in ventromedial prefrontal cortex. J Neurosci. 2014 Feb 26;34(9):3340–9.

481 Farashahi, S., Donahue, C. H., Khorsand, P., Seo, H., Lee, D., & Soltani, A. Metaplasticity as a Neural Substrate for Adaptive Learning and Choice under Uncertainty.
482 Neuron. 2017 April 19; *94*(2): 401–414.

483 FitzGerald THB, Seymour B, Dolan RJ. The role of human orbitofrontal cortex in value comparison for incommensurable objects. J Neurosci. 2009 Jul 1;29(26):8388–
484 95.

485 Friston KJ, Holmes AP, Price CJ, Büchel C, Worsley KJ. Multisubject fMRI studies and conjunction analyses. Neuroimage. 1999 Oct;10(4):385–96.

486 Garvert MM, Moutoussis M, Kurth-Nelson Z, Behrens TEJ, Dolan RJ. Learning-Induced Plasticity in Medial Prefrontal Cortex Predicts Preference Malleability. Neuron.
487 Elsevier; 2015 Jan;85(2):418–28.

488 Grill-Spector K, Henson R, Martin A. Repetition and the brain: neural models of stimulus-specific effects. Trends Cogn Sci (Regul Ed). 2006 Jan;10(1):14–23.

489 Grueschow M, Polania R, Hare TA, Ruff CC. Automatic versus Choice-Dependent Value Representations in the Human Brain. Neuron. 2015 Feb 18;85(4):874–85.

490 Hare TA, Schultz W, Camerer CF, O'Doherty JP, Rangel A. Transformation of stimulus value signals into motor commands during simple choice. Proc Natl Acad Sci
491 USA. 2011 Nov 1;108(44):18120–5.

492 Harvey BM, Klein BP, Petridou N, Dumoulin SO. Topographic representation of numerosity in the human parietal cortex. Science. 2013 Sep 6;341(6150):1123–6.

493 Hassabis, D., & Maguire, E. A. The construction system of the brain. Philosophical Transactions of the Royal Society B: Biological Sciences. 2009 May 12; 364(1521),
494 1263–1271.

495 Hayden BY, Pearson JM, Platt ML. Fictive reward signals in the anterior cingulate cortex. Science. 2009 May 15;324(5929):948–50.

496 Hayden BY, Pearson JM, Platt ML. Neuronal basis of sequential foraging decisions in a patchy environment. Nature Neuroscience. 2011 Jul;14(7):933–9.

497 Hayden BY, Platt ML. Neurons in anterior cingulate cortex multiplex information about reward and action. J Neurosci. 2010 Mar 3;30(9):3339–46.

498 Howard JD, Gottfried JA, Tobler PN, Kahnt T. Identity-specific coding of future rewards in the human orbitofrontal cortex. Proceedings of the National Academy of
499 Sciences. 2015 Apr 21;112(16):5195–200.

500 Hunt LT, Behrens TEJ, Hosokawa T, Wallis JD, Kennerley SW. Capturing the temporal evolution of choice across prefrontal cortex. eLife Sciences. 2015;4.

501 Hunt LT, Dolan RJ, Behrens TEJ. Hierarchical competitions subserving multi-attribute choice. Nature Neuroscience. Nature Publishing Group; 2014 Oct 12;:1–14.

502 Hunt LT, Kolling N, Soltani A, Woolrich MW, Rushworth MFS, Behrens TEJ. Mechanisms underlying cortical activity during value-guided choice. Nature Neuroscience.
503 2012 Jan 8;15(3):470–6–S1–3.

504 Jacob SN, Nieder A. Notation-Independent Representation of Fractions in the Human Parietal Cortex. J Neurosci. 2009 Apr 8;29(14):4652–7.

505 Jocham, G., Furlong, P. M., Kröger, I. L., Kahn, M. C., Hunt, L. T., & Behrens, T. E. J. Dissociable contributions of ventromedial prefrontal and posterior parietal cortex
506 to value-guided choice. NeuroImage. 2014 Oct 15; 100(C), 498–506.

507 Kable JW, Glimcher PW. The neural correlates of subjective value during intertemporal choice. Nature Neuroscience. 2007 Dec;10(12):1625–33.

508 Kahnt T, Heinzle J, Park SQ, Haynes JD. The neural code of reward anticipation in human orbitofrontal cortex. Proceedings of the National Academy of Sciences. 2010
509 Mar 30;107(13):6010–5.

510 Kahnt T, Heinzle J, Park SQ, Haynes JD. Decoding the Formation of Reward Predictions across Learning. J Neurosci. 2011 Oct 12;31(41):14624–30.

511 Kanayet FJ, Opfer JE, Cunningham WA. The Value of Numbers in Economic Rewards. Psychol Sci. 2014 Aug 6;25(8):1534–45.

512 Kennerley SW, Behrens TEJ, Wallis JD. Double dissociation of value computations in orbitofrontal and anterior cingulate neurons. Nature Neuroscience. 2011 Oct
513 30;14(12):1581–9.

514 Klein-Flügge MC, Barron HC, Brodersen KH, Dolan RJ, Behrens TEJ. Segregated Encoding of Reward-Identity and Stimulus-Reward Associations in Human
515 Orbitofrontal Cortex. J Neurosci. 2013 Feb 13;33(7):3202–11.

516 Knutson B, Rick S, Wimmer GE, Prelec D, Loewenstein G. Neural predictors of purchases. Neuron. 2007 Jan 4;53(1):147–56.

517 Kolling N, Behrens TEJ, Mars RB, Rushworth MFS. Neural mechanisms of foraging. Science. 2012 Apr 6;336(6077):95–8.

518 Kolling N, Wittmann M, Rushworth MFS. Multiple neural mechanisms of decision making and their competition under changing risk pressure. Neuron. 2014 Mar
519 5;81(5):1190–202.

520 Kolling, N., Behrens, T., Wittmann, M. K., & Rushworth, M. Multiple signals in anterior cingulate cortex. Current Opinion in Neurobiology. 2016 April; 37, 36–43.

521 Krajbich I, Armel C, Rangel A. Visual fixations and the computation and comparison of value in simple choice. Nature Neuroscience. 2010 Oct;13(10):1292–8.

522 Lebreton M, Jorge S, Michel V, Thirion B, Pessiglione M. An automatic valuation system in the human brain: evidence from functional neuroimaging. Neuron. 2009
523 Nov 12;64(3):431–9.

524 Levy I, Lazzaro SC, Rutledge RB, Glimcher PW. Choice from non-choice: predicting consumer preferences from blood oxygenation level-dependent signals obtained
525 during passive viewing. Journal of Neuroscience. 2011 Jan 5;31(1):118–25.

526 Liljeholm M, Tricomi E, O'Doherty JP, Balleine BW. Neural correlates of instrumental contingency learning: differential effects of action-reward conjunction and
527 disjunction. J Neurosci. 2011 Feb 16;31(7):2474–80.

528 Lim S-L, O'Doherty JP, Rangel A. Stimulus value signals in ventromedial PFC reflect the integration of attribute value signals computed in fusiform gyrus and
529 posterior superior temporal gyrus. J Neurosci. 2013 May 15;33(20):8729–41.

530 Loffler G, Yourganov G, Wilkinson F, Wilson HR. fMRI evidence for the neural representation of faces. Nature Neuroscience. 2005 Oct;8(10):1386–90.

531 Lopatina N, McDannald MA, Styer CV, Sadacca BF, Cheer JF, Schoenbaum G. Lateral orbitofrontal neurons acquire responses to upshifted, downshifted, or blocked
532 cues during unblocking. eLife Sciences. 2015;4.

533 Louie K, Grattan LE, Glimcher PW. Reward Value-Based Gain Control: Divisive Normalization in Parietal Cortex. J Neurosci. 2011 Jul 20;31(29):10627–39.

534 Lucantonio F, Gardner MPH, Mirenzi A, Newman LE, Takahashi YK, Schoenbaum G. Neural Estimates of Imagined Outcomes in Basolateral Amygdala Depend on
535 Orbitofrontal Cortex. J Neurosci. 2015 Dec 16;35(50):16521–30.

536 McComb K, Packer C, Pusey A. Roaring and numerical assessment in contests between groups of female lions, Panthera leo. Animal Behaviour. Academic Press;
537 1994 Feb;47(2):379–87.

538 McNamee D, Rangel A, O'Doherty JP. Category-dependent and category-independent goal-value codes in human ventromedial prefrontal cortex. Nature
539 Neuroscience; 2013 Feb 17;16(4):479–85.

540 Medic N, Ziauddeen H, Vestergaard MD, Henning E, Schultz W, Farooqi IS, et al. Dopamine modulates the neural representation of subjective value of food in hungry
541 subjects. J Neurosci. 2014 Dec 10;34(50):16856–64.

542 Mnih V, Kavukcuoglu K, Silver D, Rusu AA, Veness J, Bellemare MG, et al. Human-level control through deep reinforcement learning. Nature. 2015 Feb
543 26;518(7540):529–33.

544 Montague PR, Berns GS. Neural Economics and the Biological Substrates of Valuation. Neuron. 2002 Oct;36(2):265–84.

545 Nieder A. The neuronal code for number. Nature Reviews Neuroscience. 2016.

546 Nieder A, Freedman DJ, Miller EK. Representation of the quantity of visual items in the primate prefrontal cortex. Science. 2002 Sep 6;297(5587):1708–11.

547 Nieder A, Miller EK. A parieto-frontal network for visual numerical information in the monkey. Proc Natl Acad Sci USA. 2004 May 11;101(19):7457–62.

548 Noonan, M. P., Mars, R. B., & Rushworth, M. F. S. Distinct roles of three frontal cortical areas in reward-guided behavior. The Journal of Neuroscience. 2011 Oct 5;
549 31(40), 14399–14412.

550 O'Doherty J, Kringelbach ML, Rolls ET, Hornak J, Andrews C. Abstract reward and punishment representations in the human orbitofrontal cortex. Nature
551 Neuroscience. 2001 Jan;4(1):95–102.

552 O'Doherty JP. The problem with value. Neurosci Biobehav Rev. 2014 Jun;43:259–68.

553 O'Reilly JX, Schüffelgen U, Cuell SF, Behrens TEJ, Mars RB, Rushworth MFS. Dissociable effects of surprise and model update in parietal and anterior cingulate cortex.
554 Proceedings of the National Academy of Sciences. 2013 Sep 17;110(38):E3660–9.

555 Padoa-Schioppa C. Neurobiology of economic choice: a good-based model. Annual Review of Neuroscience. 2011;34:333–59.

556 Padoa-Schioppa C, Assad JA. Neurons in the orbitofrontal cortex encode economic value. Nature. 2006 Apr 23;441(7090):223–6.

557 Padoa-Schioppa C, Assad JA. The representation of economic value in the orbitofrontal cortex is invariant for changes of menu. Nature Neuroscience. 2008
558 Jan;11(1):95–102.

559 Padoa-Schioppa C, Schoenbaum G. Dialogue on economic choice, learning theory, and neuronal representations. Current Opinion in Behavioral Sciences. 2015
560 Oct;5:16–23.

561 Paz, R., Bauer, E. P., & Paré, D. Theta synchronizes the activity of medial prefrontal neurons during learning. Learning & Memory (Cold Spring Harbor, N.Y.). 2008
562 July; 15(7), 524–531.

563 Pessiglione M, Seymour B, Flandin G, Dolan RJ, Frith CD. Dopamine-dependent prediction errors underpin reward-seeking behaviour in humans. Nature. 2006 Aug
564 23;442(7106):1042–5.

565 Piazza M, Izard V, Pinel P, Le Bihan D, Dehaene S. Tuning curves for approximate numerosity in the human intraparietal sulcus. Neuron. 2004 Oct 28;44(3):547–55.

566 Piazza M, Pinel P, Le Bihan D, Dehaene S. A magnitude code common to numerosities and number symbols in human intraparietal cortex. Neuron. 2007 Jan
567 18;53(2):293–305.

568 Pinel P, Piazza M, Le Bihan D, Dehaene S. Distributed and overlapping cerebral representations of number, size, and luminance during comparative judgments.
569 Neuron. 2004 Mar 25;41(6):983–93.

570 Plassmann H, O'Doherty J, Rangel A. Orbitofrontal cortex encodes willingness to pay in everyday economic transactions. J Neurosci. 2007 Sep 12;27(37):9984–8.

571 Polania R, Krajbich I, Grueschow M, Ruff CC. Neural Oscillations and Synchronization Differentially Support Evidence Accumulation in Perceptual and Value-Based
572 Decision Making. Neuron. 2014 May;82(3):709–20.

573 Price CJ. A review and synthesis of the first 20years of PET and fMRI studies of heard speech, spoken language and reading. Neuroimage. Elsevier Inc; 2012 Aug
574 15;62(2):816–47.

575 Rahman NA, Fadzly N, Dzakwan NM, Zulkifli NH. The Numerical Competency of Two Bird Species (Corvus splendens and Acridotheres tristis). Tropical Life Sciences
576 Research. School of Medical Sciences, Universiti Sains Malaysia; 2014 Aug 1;25(1):95.

577 Ramirez-Cardenas A, Moskaleva M, Nieder A. Neuronal Representation of Numerosity Zero in the Primate Parieto-Frontal Number Network. Current Biology.
578 Elsevier; 2016 Apr;26(10):1285–94.

579 Rogers RD, Owen AM, Middleton HC, Williams EJ, Pickard JD, Sahakian BJ, et al. Choosing between small, likely rewards and large, unlikely rewards activates inferior
580 and orbital prefrontal cortex. J Neurosci. 1999 Oct 15;19(20):9029–38.

581 Rugani R, Fontanari L, Simoni E, Regolin L, Vallortigara G. Arithmetic in newborn chicks. Proc Biol Sci. 2009 Jul 7;276(1666):2451–60.

582 Rushworth MFS, Behrens TEJ. Choice, uncertainty and value in prefrontal and cingulate cortex. Nature Neuroscience. Nature Publishing Group; 2008 Mar
583 26;11(4):389–97.

584 Rutledge RB, Dean M, Caplin A, Glimcher PW. Testing the reward prediction error hypothesis with an axiomatic model. J Neurosci. 2010 Oct 6;30(40):13525–36.

585 Rutledge RB, Skandali N, Dayan P, Dolan RJ. A computational and neural model of momentary subjective well-being. Proceedings of the National Academy of
586 Sciences. 2014 Aug 19;111(33):12252–7.

587 Schuck NW, Cai MB, Wilson RC, Niv Y. Human Orbitofrontal Cortex Represents a Cognitive Map of State Space. Neuron. 2016 Sep 21;91(6):1402–12.

588 Schultz W, Dayan P, al E. A neural substrate of prediction and reward. Science. 1997.

589 Schultz W, O'Neill M, Tobler PN, Kobayashi S. Neuronal signals for reward risk in frontal cortex. Annals of the New York Academy of Sciences. 2011 Dec
590 6;1239(1):109–17.

591 Seo H, Lee D. Temporal filtering of reward signals in the dorsal anterior cingulate cortex during a mixed-strategy game. J Neurosci. 2007 Aug 1;27(31):8366–77.

592 Silver D, Huang A, Maddison CJ, Guez A, Sifre L, van den Driessche G, et al. Mastering the game of Go with deep neural networks and tree search. Nature. 2016 Jan
593 28;529(7587):484–9.

594 Stalnaker TA, Cooch NK, McDannald MA, Liu T-L, Wied H, Schoenbaum G. Orbitofrontal neurons infer the value and identity of predicted outcomes. Nat Comms.
595 2014;5:3926.

596 Stalnaker TA, Cooch NK, Schoenbaum G. What the orbitofrontal cortex does not do. Nature Neuroscience. 2015 May;18(5):620–7.

597 Strait, C. E., Blanchard, T. C., & Hayden, B. Y. Reward value comparison via mutual inhibition in ventromedial prefrontal cortex. Neuron. 2014 Jun 18; *82*(6), 1357–
598 1366.

599 Summerfield C, Trittschuh EH, Monti JM, Mesulam M-M, Egner T. Neural repetition suppression reflects fulfilled perceptual expectations. Nature Neuroscience. 2008
600 Sep;11(9):1004–6.

601 Sutton RS, Barto AG. Reinforcement learning: An introduction. MIT Press, Cambridge; 1998.

602 Takahashi YK, Chang CY, Lucantonio F, Haney RZ, Berg BA, Yau H-J, et al. Neural estimates of imagined outcomes in the orbitofrontal cortex drive behavior and
603 learning. Neuron. 2013 Oct 16;80(2):507–18.

604 Tom SM, Fox CR, Trepel C, Poldrack RA. The Neural Basis of Loss Aversion in Decision-Making Under Risk. Science. 2007 Jan 26;315(5811):515–8.

605 Wang X-J. Decision making in recurrent neuronal circuits. Neuron. 2008 Oct 23;60(2):215–34.

606 Weiskopf N, Hutton C, Josephs O, Deichmann R. Optimal EPI parameters for reduction of susceptibility-induced BOLD sensitivity losses: A whole-brain analysis at 3 T
607 and 1.5 T. Neuroimage. 2006 Nov;33(2):493–504.

608 Wilson RC, Takahashi YK, Schoenbaum G, Niv Y. Orbitofrontal Cortex as a Cognitive Map of Task Space. Neuron. 2014 Jan;81(2):267–79.

609 Wright ND, Symmonds M, Dolan RJ. Distinct encoding of risk and value in economic choice between multiple risky options. Neuroimage. 2013 Nov 1;81:431–40.

610 Wunderlich K, Dayan P, Dolan RJ. Mapping value based planning and extensively trained choice in the human brain. Nature Neuroscience. Nature Publishing Group.
611 Nature Publishing Group; 2012 Mar 11;15(5):786–91.

612 Xie J, Padoa-Schioppa C. Neuronal remapping and circuit persistence in economic decisions. Nature Neuroscience. 2016 Jun;19(6):855–61.

613 Zysset S, Wendt CS, Volz KG, Neumann J, Huber O, Cramon von DY. The neural implementation of multi-attribute decision making: a parametric fMRI study with
614 human subjects. Neuroimage. 2006 Jul 1;31(3):1380–8.

615

616 ## Captions

617 **Figure 1 | Experimental procedure (A)** We used giftcards to manipulate quality and quantity. Cards from different shops had different qualities,
618 depending upon the subjective value of money that can be spent at that shop alone. Quantity varied as the amount of money (number of £)
619 depicted on the card. **(B)** Following an initial behavioural session in which we mapped value functions for different giftcards, a subset of
620 participants were invited to return for an fMRI session. **(C)** Behavioural experiment. The first task involved an auction procedure (Becker-DeGroot-
621 Marschak procedure, BDM). Participants were offered different cards with varying amounts of money on them, and indicated the maximum
622 amount they would be willing to pay for that card. In the second (paired choice) task, subjects made choices between pairs of giftcards with equal

quantities (£20). **(D)** fMRI experiment. On most trials (6 of 7) participants saw only a single giftcard from one of three different shops, with a randomly varying quantity (amount of money). On decision trials (1 of 7), a second giftcard was displayed 2s after the first, and participants had 4s to make a choice between the two giftcards. ITI's were normally distributed around 1.5s.

Figure 2 | Example participants from behavioural experiment We used data from the behavioural session to determine subsequent inclusion in an fMRI study based on criteria of consistency and diversity of preferences for different giftcards (assessed using the predictability of BDM ratings), relationships between BDM and paired choice tasks, and correlations between quantity and subjective value. **(A)** Firstly, we examined quantity-bid relationships for the 13 different giftcards. The slope of the quantity-bid relationship for each giftcard is a measure of that giftcard's quality, with higher slopes corresponding to more valuable brands. Here, participant i has diverse but noisy preferences, ii is consistent but has similar preferences across giftcards, whilst iii display an acceptable level of consistency whilst maintaining diverse preferences. **(B)** To assess preference stability, we compared the slope of lines estimated from the BDM task with the number of times each giftcard was chosen in the paired-choice task. Participant i shows a weak relationship between choices in each session; ii is consistent but shows little variability; and iii is both consistent and displays diverse preferences. **(C)** For the fMRI experiment, we selected three giftcards for each participant that differed maximally in quality. Here we show BDM plots for selected cards. As before, i is noisy but shows diverse quality preferences, ii has similar preferences over giftcards, and iii has consistent and diverse preferences over giftcards.

Figure 3 | Behavioural results for subjects in scanning experiment (A) Average quantity-bid functions show the difference in quality for three selected giftcards for subjects who completed both the behavioural and fMRI sessions (n=25). **(B)** In a pre-scanning paired-choice session, we confirmed that the ordering of cards by quality was highly consistent between sessions. **(C)** Analysis of choices made in the MRI scanner. During the fMRI experiment, participants made 48 choices between cards of varying quality and quantity (see Figure 1D). We used the differences between options to predict choices using logistic regression. The differences between options in both quality (T_{24}=8.6, $p<0.001$) and quantity (T_{24}=13.7,$p<0.001$) were predictive of choice. Importantly, the interaction between quality and quantity also predicted choice (T_{24}=3.8,$p<0.001$), consistent with the multiplicative relationship expected from the observed quantity-utility functions (Figure 3A).

Figure 4 | Representation of quality, quantity, and their interaction (A) We observed bilateral coding of offer quality [$Quality_{High} - Quality_{Low}$] bilaterally in the Inferior Frontal Gyrus (IFG). **(B)** Increasing quantity, as tested by [$Quantity_{HighQuality} + Quantity_{MediumQuality} + Quantity_{LowQuality}$], was associated with greater activity bilaterally in the Intra Parietal Sulcus (IPS). **(C)** Activations in the posterior cingulate cortex were consistent with representing the interaction of quality and quantity but not either variable separately [$Quantity_{HighQuality} - Quantity_{LowQuality}$]. Errors bars are SEM across subjects, SPMs thresholded at $p<0.01$ for visualization.

Figure 5 | Computation of value from component parts in the anterior cingulate cortex (A) Overlapping effects of quality, quantity, and their interaction in the ACC. A conjunction analysis revealed overlapping representations of each component ($p<0.05_{uncorrected}$) [green] in the ACC, suggesting a nexus for the computation of value. A complementary analysis using an explicit representation of integrated value as a parametric modulator identified the same region ($p<0.05_{FWE\text{-}corrected}$) [turquoise]. Timecourse displayed for illustration purposes. **(B)** Decision > Non-Decision trials. The ACC also showed higher activity in trials upon which a decision was made compared to valuation trials [red], overlapping with the conjunction analysis identified in panel a [green]. **(C)** Participants with stronger representations of quality in the IFG showed stronger representations of quality in the ACC (r=0.63, $p<0.001$). **(D)** Quality sensitivity in IFG was unrelated to quantity coding in ACC (r=0.04, p=0.83). **(E)** Quantity sensitivity in IPS was unrelated to quality coding in ACC (r=-0.14, p=0.50). **(F)** Participants with stronger representations of quantity in the IPS showed stronger representations of quantity in the ACC (r=0.68, $p<0.001$). Each point is one participant.

Figure 6 | Neural quantity sensitivity relate to choice predictability We found that coefficients for quantity in **(A)** IPS (ρ=0.60, p=0.002) and **(B)** the ACC (ρ=0.42, p=0.039) correlated with the predictability of participants' choices, as assessed by the ability of our logistic regression model to predict choice. Correlations with quality coding in the IFG (ρ=0.41, p=0.104) and ACC (ρ=0.30, p=0.142) were positive but not significant.

Figure 7 | Repetition suppression for value in the anterior cingulate cortex (A) Repetition suppression analysis logic. We hypothesize a population of neurons tuned to value where the different neurons have overlapping tuning curves spanning the range of values presented. Black arrows denote stimulus value for that trial. If consecutive trials activate non-overlapping populations of neurons, evoked responses for each stimulus are similarly high on each trial (top panel in orange). However, repeated presentation of the same stimulus produces repeated activation of the same neurons on consecutive trials, leading to a reduction in the neural response (bottom panel in blue). Summation over all neurons in the population (as in the BOLD signal measured in fMRI), leads to higher activity when consecutive stimuli activate unique subsets of neurons (top panel) than when consecutively activated populations overlap (bottom panel). Predicted BOLD activity is thus proportional to the absolute difference in value between consecutive trials. **(B)** Evidence for multiple forms of value coding in the cingulate. We examined cingulate representations of repetition suppression to integrated value (change in value from trial n-1 to trial n, ΔIntegratedValue) [green], and monotonic encoding of integrated value (a standard parametric modulator approach) [red]. Voxels sensitive to repetition suppression were more posterior, with monotonic encoding stronger in anterior voxels. **(C)** The ACC region identified in the conjunction analysis (Figure 5A) also shows repetition suppression to integrated value. We extracted mean parameter estimates for ΔIntegratedValue and for integrated value from the voxels identified in the conjunction analysis. Both were positive on average (ΔIntegratedValue: T_{24}=2.48,p=0.020; Integrated Value: T=3.26, p=0.0034). Error bars are SEM across participants.

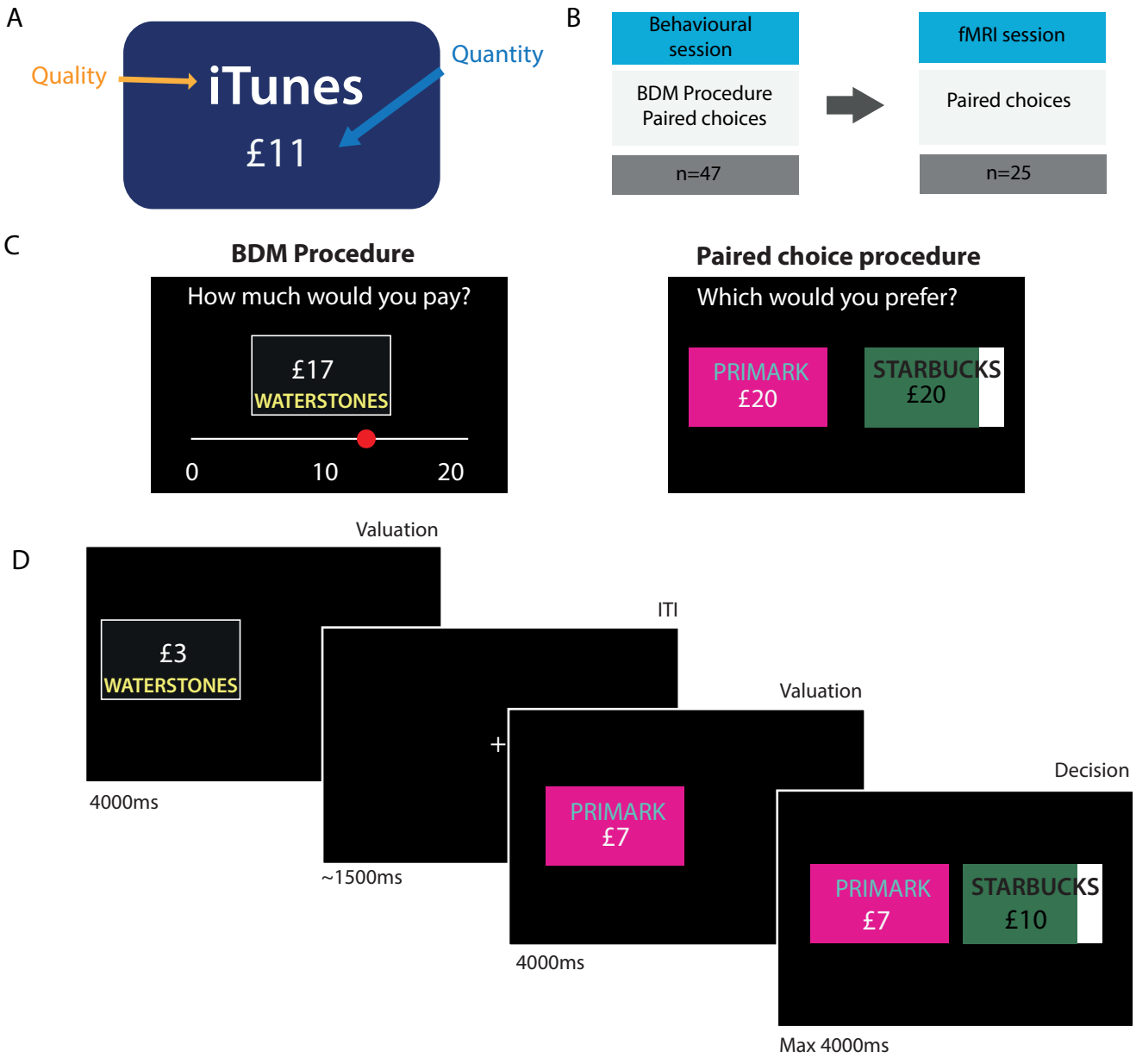

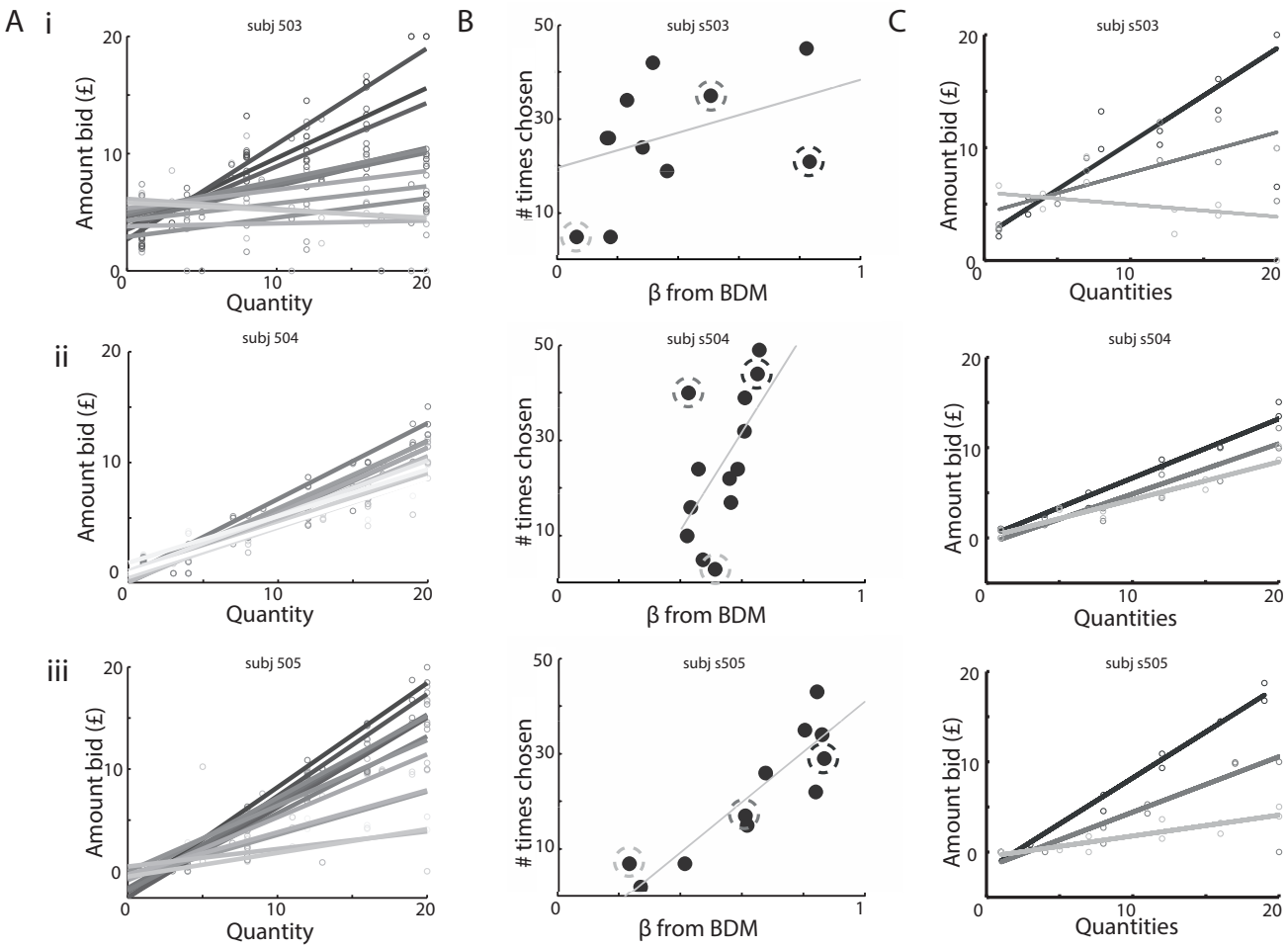

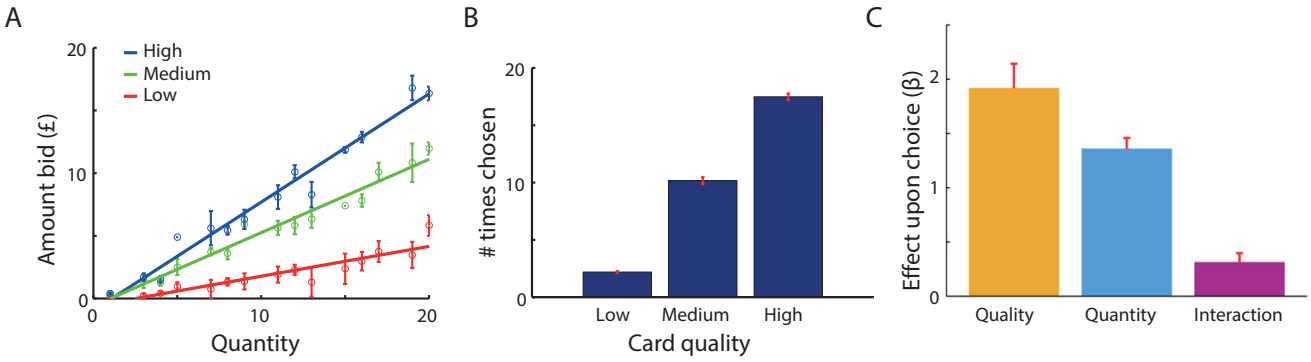

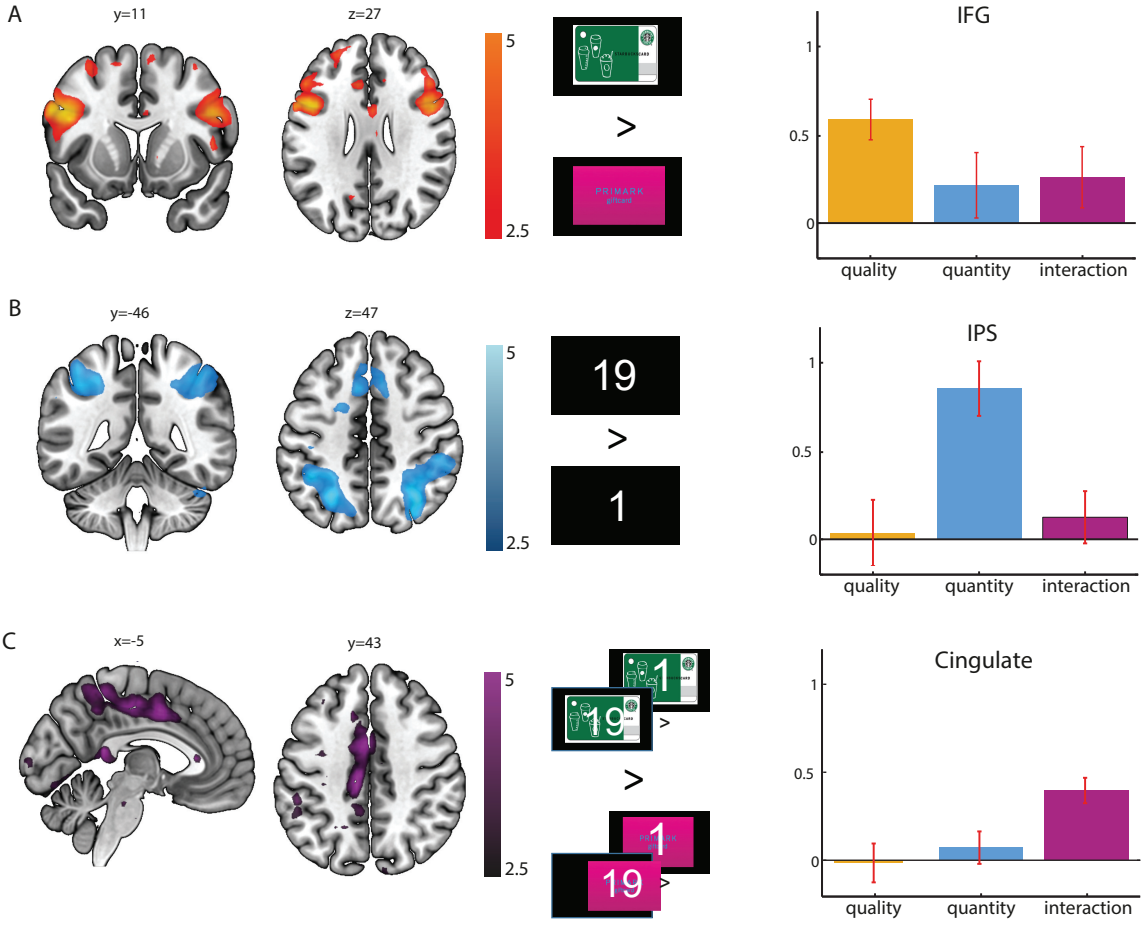

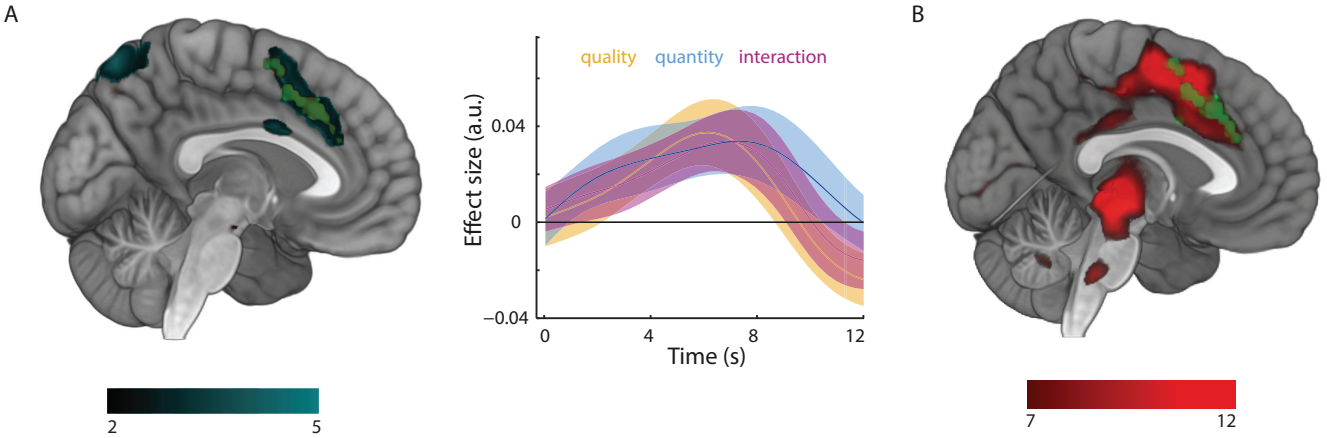

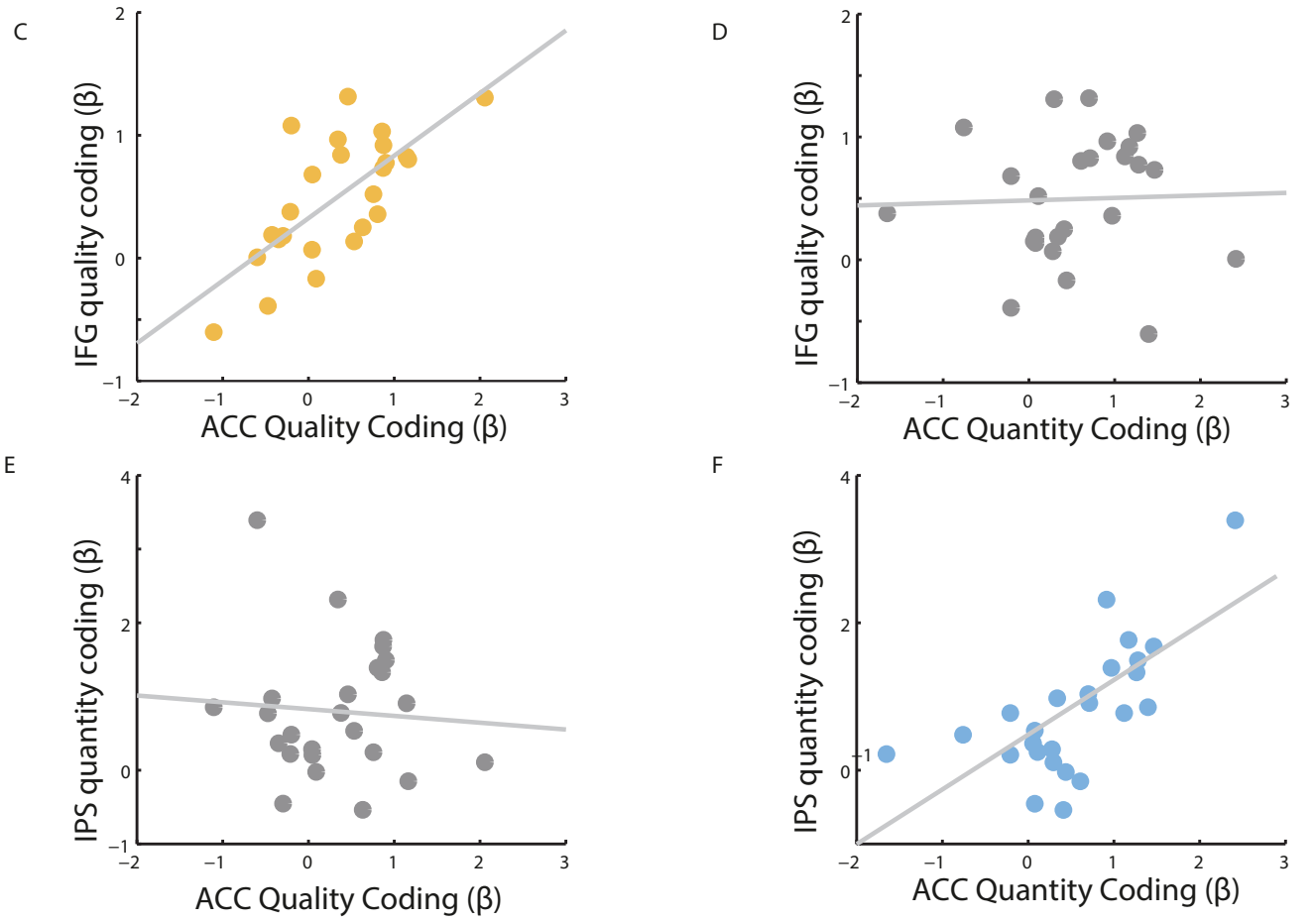

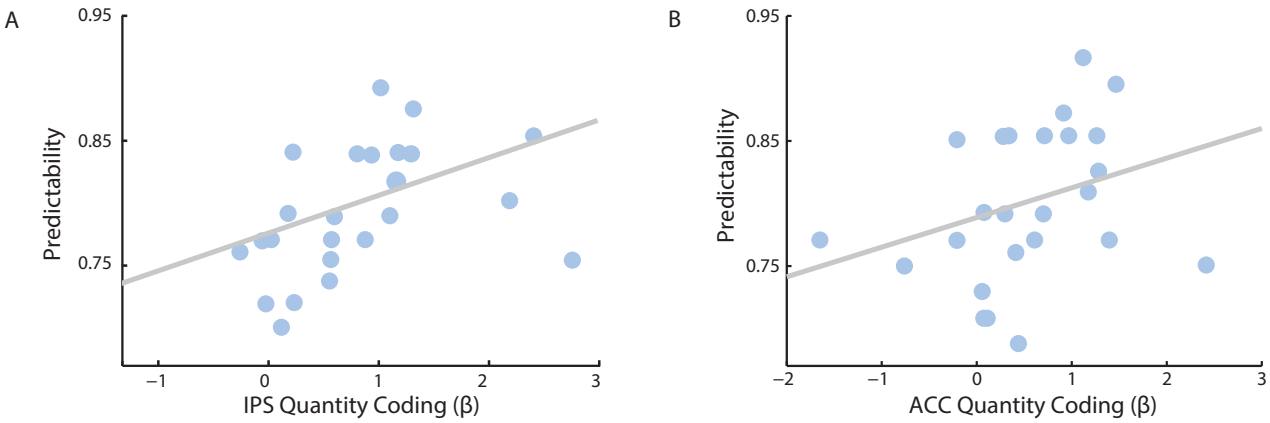

A

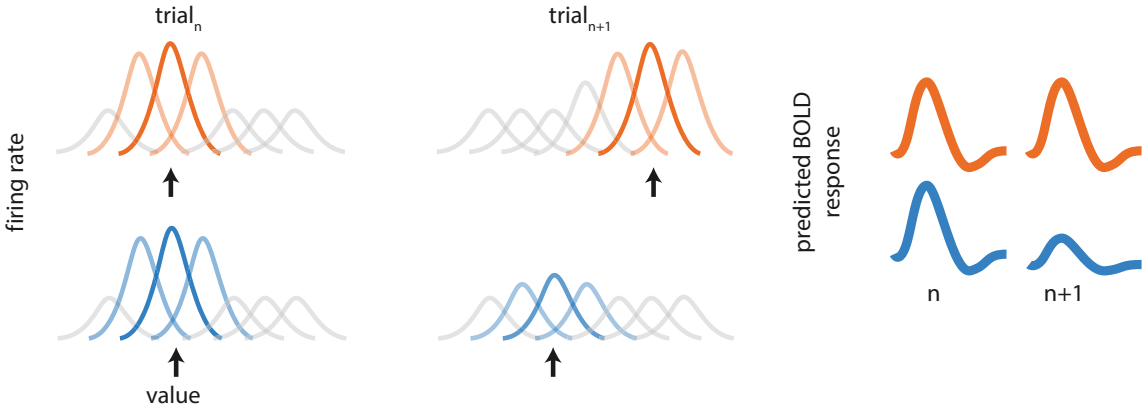

B

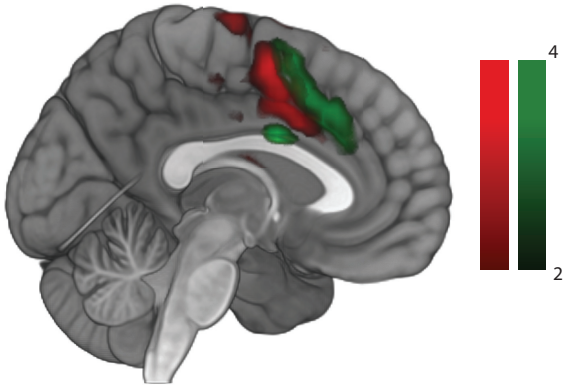

C